

AD-A241 758



RED 5653-1H-01

(2)

CHAOTIC BEHAVIOUR IN QUANTUM DYNAMICS

Final Technical Report

DTIC  
ELECTE  
OCT 16 1991  
S D D

by

G. Casati, I. Guarneri

September 1991

United States Army

EUROPEAN RESEARCH OFFICE OF THE U.S. ARMY

London England

CONTRACT NUMBER DAJA45-88-C-0003

Centro di Cultura Scientifica "A. Volta"

Villa Olmo - 22100 Como - Italy

Approved for Public Release; distribution unlimited

91-13241



## 1-BACKGROUND: REVIEW OF BASIC CONCEPTS.

1.1- Chaos in microphysics?

1.2- Dynamical Localization

## 2-STATEMENT OF PROBLEMS.

## 3- THE HYDROGEN ATOM IN A MICROWAVE FIELD.

3.1- The 1-d model for microwave excitation

3.2- The Kepler Map

3.3- The Quantum Kepler Map

3.4- Localization in the Quantum Kicked Rotator

3.5- Localization in the H-atom

3.6- Delocalization

3.7- Numerical Checks

3.8- Beyond the 1d Model

3.9- Experimental Verifications

## 4- HIGHER DIMENSIONAL LOCALIZATION

4.1- Anderson transition in a dynamical model

## 5- CONCLUSIONS AND RECOMMENDATIONS

## 6- FIGURE CAPTIONS

## 7- BIBLIOGRAPHY

Accession For	
NTIS CRA&I	<input checked="" type="checkbox"/>
DTIC TAB	<input type="checkbox"/>
Unannounced	<input type="checkbox"/>
Justification	
By	
D t o	
A t t e s t	
D s t	
A-1	



## 1.- BACKGROUND; REVIEW OF BASIC CONCEPTS.

This final report illustrates the results of a three-years research program on Quantum Chaos.

After some ten years of investigations on the quantum dynamics of classically chaotic systems, the basic question whether in quantum mechanics anything survives of the impressive manifestations of classical chaos hasn't yet been given a clear answer. If a general indication is to be drawn from the analytical, numerical and experimental results up to now obtained, this is that classical chaos is suppressed or at least strongly inhibited by quantization; as a consequence, "quantum chaos" - a widespread denomination for this research area - is still sometimes considered a questionable concept. In spite of this negative remark, the search for quantum manifestations of classical chaos has led to substantial advance in several areas of microphysics: semiclassical methods have been substantially refined and new phenomenological aspects of the dynamics of small quantum systems have been identified.

### 1.1-Chaos in microphysics?

A major impulse to the investigations reported below was given by the analysis of some specific models used in various areas of microphysics. From the standpoint of classical mechanics, these models exhibit the typical features of nonlinear Hamiltonian systems and under appropriate conditions they enter a chaotic regime. The question is, how is the classical chaos mirrored in the quantum dynamics of these models?

This is a very important question for the present day physics, both from a theoretical and an applicative viewpoint. On theoretical grounds, it involves the nature of the semiclassical approximation when the classical motion is chaotic, i.e, in a situation in which the boundary between quantum and classical mechanics is still vague and undefined so many years after the birth of quantum mechanics.

On more physical grounds, the onset of classical chaos is often accompanied by

strong instabilities that lead to experimentally observable and often dramatic behavior. The possibility that this sort of phenomena can be observed in microphysics, i.e. in the domain of validity of quantum mechanics, opens a vast new field to experimental research. A widely investigated example ( to be discussed in more detail below ), to which the work reported here has given essential contributions, is that of an atom in an external radiation field. This involves the study of the dynamics of an electron in the combined Coulomb plus radiation field, and a simple model for that is a nonlinear oscillator subject to an external perturbation periodic in time. Such a classical model turns out to exhibit a transition to chaos as soon as the perturbation strength reaches a critical value. Were the atom a classical object, in such conditions it would be rapidly ionized (*chaotic ionization*). The atom however is quantum, so the important question arises: does quantum mechanics allow for any such ionization mechanism?

According to experimental and theoretical results, it does - under certain conditions at least. Nevertheless, the modifications that quantum mechanics imposes over the classical chaotic picture are extremely important and their investigation has opened a new field to both theoretical and experimental analysis.

## 1.2-Dynamical localization

The concept of *dynamical localization* dominates the present-day understanding of quantum chaos in periodically perturbed systems. A classical nonlinear oscillator subject to an external perturbation periodic in time can enter a regime of chaotic motion marked by diffusive growth of its energy. The motion of such an oscillator becomes very erratic and looks very much like a random walk; in that case, only a statistical description proves viable ( though the system is, in principle, perfectly deterministic and has just a very few freedoms ). This kind of a motion is called *chaotic diffusion*.

Chaotic diffusion is a physically important aspect of classical chaos. Chaotic instability leads to this type of response, e.g., in nonlinear systems subjected to periodic perturbations. This type of instability is well known in classical dynamics and is often responsible for undesirable effects in macroscopic systems.

The stability of atoms or molecules in external fields clearly depends on whether this phenomenon survives at least in part at the quantum level. It turns out that quantization has a strong effect on this diffusion. As a matter of fact, the study of a simple albeit abstract model ( the so-called Kicked Rotator ) yielded the remarkable result, that quantization strongly limits and even suppresses this type of diffusion. In other words, a classical system would continue to absorb energy from the external perturbing field, but its quantum version is much more stable and reaches after a while a sort of steady-state in which no energy is further absorbed ( in the average ).

The mechanism that produces this quantum quenching of the classical diffusive behaviour is basically quantum interference.

In the chaotic regime, the classical oscillator would display a host of different orbits that behave quite differently in spite of the closeness of their starting points ( initial conditions ); in the quantum case, all these wildly different dynamical possibilities *interfere*, thus leading the process of excitation to a halt.

This phenomenon has been recognized to be analogous to the Anderson localization of Solid State Physics. <sup>1</sup>

At very low temperatures, the resistance offered by a crystalline solid to the motion of electrons is essentially due to imperfections in the crystal structure, that spoil its perfect periodicity. The Anderson model is a model for the study of the residual resistance, in which the electron jumps from one site to another in a disordered lattice - i.e., a lattice that exhibits random deviations from the perfect crystal periodicity. Classically a random walk would be expected, but quantum mechanically it turns out that the diffusion of the particle through the disordered lattice is stopped or at least inhibited by interference ( depending on the spatial dimension of the lattice ). Due to this effect, the residual conductance of a linearly shaped sample of a crystalline solid decreases exponentially with the length of the sample. The rate of exponential decay  $\gamma$  across a given sample depends on the specific sample ; in the Anderson and related models, the lattice imperfections are described by a random potential, so that the actual rate of decay depends on the particular realization of that random potential. However,

in the limit of an infinitely long sample  $\gamma$  turns out to be realization-independent and its inverse  $\gamma^{-1}$  is known as the *localization length*.

Realizing that the effect of quantization on classical chaotic diffusion and the Anderson localization are just different manifestations of a common quantum dynamical effect was the starting point of a theory known as *dynamical localization theory*. At the heart of this theory lies the assumption that this effect is a generic occurrence in the quantum dynamics of systems that classically would display a chaotic diffusion, and that it can be efficiently analyzed by means of the same methods used in the theory of Anderson localization. This means that the dynamics should be analyzed on statistical grounds. In other words, the theory should give up a complete description of all the details of the quantum dynamics; only certain important average quantities like the localization lengths should be taken into account.

The link of the dynamical localization effect with the Anderson localization can also be qualitatively understood as follows. A quantum system subjected to some external monochromatic field will perform a chain of transitions between his energy levels by absorbing or releasing quanta of the field. If the energy of one quantum is larger than the typical level spacing, and provided that the width of one such one-photon transition is not too large, then, during its time evolution, the system will significantly populate only narrow resonant zones around the levels that can be reached by absorbing or releasing an integer number of quanta starting from the initially excited levels. The motion will thus resemble that of a particle on a discrete lattice, each site in the lattice representing a particular quasi-resonant level. A jump from one site to another will correspond to absorption or release of some photons. If the levels were exactly resonant with one another, the sites should be evenly spaced in energy by exactly one quantum and should make up a periodic lattice, but this will not be the typical case. In general, every quasi-resonant level will have a detuning from exact resonance; therefore all the sites in the resonant lattice will be more or less displaced from the ideal resonant configuration and will make up a sort of a disordered lattice.

This picture of the dynamics of the driven quantum systems is oversimplified but

it brings to the light the origin of dynamical localization. Indeed, provided that the sequence of detunings can be assumed to be irregular enough, a formal identification with models of the Anderson type is possible. In that case, no unlimited escape along the quasi-resonant lattice is to be expected - this possibility will be ruled out by interference.

## 2.- STATEMENT OF PROBLEMS

Is this quantum suppression a general phenomenon?

At the core of the so-called "dynamical localization theory" lies the idea that an inhibition of diffusive excitation due to quantum interference should be expected in wide generality, upon quantizing a classical system in which a chaotic diffusion takes place. This surmise, supported by extensive numerical simulations and by some heuristic arguments, led to the physically important prediction, that the quantum suppression of classical chaos should be observed also in the case of a H-atom in a microwave field.<sup>2,3</sup> This would result in significantly smaller ionization rates than classically expected. The problems we addressed in our investigations were therefore

- (i) under what conditions - if any - can the localization effect be observed in the dynamics of real hydrogen atoms in microwave fields; being aimed at detecting the effect in laboratory experiments, this part of our program involved a careful numerical simulation of the actually realizable experimental conditions;
- (ii) how can the localization effect be circumvented, giving rise to a mechanism of fast unbounded excitation eventually leading to ionization,
- (iii) how far the similarity between the dynamical localization and the Anderson localization can be pushed, and to what extent, can already known theoretical results about the latter be used to describe the dynamics of classically chaotic systems such as atoms or molecules in radiation fields.

### 3.-THE HYDROGEN ATOM IN A MICROWAVE FIELD

The problem of microwave ionization of hydrogen atoms has played an extremely important role in the development of "quantum chaos", because it offers a unique opportunity for experimentally investigating the relevance of classical chaos in quantum mechanics. The behavior of the atom in the microwave field can be theoretically and numerically analyzed on a very simple model of a periodically driven nonlinear oscillator. In the classical model the onset of chaos provides a very efficient ionization mechanism: for any initial state of the atom there is a critical field strength above which the classical trajectories become chaotic and the atom starts absorbing energy in a diffusive way. This diffusive excitation eventually leads to ionization. The theory of dynamical localization has been applied to the problem of a hydrogen atom in a microwave field and has led to an interesting prediction, that has been successfully checked in laboratory experiments, as explained below.<sup>2,3,4</sup> Though in some appropriate frequency range the process of ionization of the atom is just as strong as the classical chaotic picture would predict, at higher frequency quantum interference comes into play and inhibits the ionization process.

#### 3.1.- The 1-d model for microwave excitation

The most widely studied model for the behaviour of H-atoms in microwave fields is that of an electron moving on the half line  $x \geq 0$  (parallel to the direction of the electric field). The Hamiltonian ( in atomic units ) is:

$$H = \frac{p^2}{2} - \frac{1}{x} + \epsilon x \cos \omega t \quad (1)$$

and is supplemented with a condition of elastic reflection at  $x = 0$ . In principle, the 1d model is justified only for special choices of the initial states ( extremal Stark levels ), but numerical simulations of the model have given surprisingly good data for the onset of ionization in 3d experiments<sup>5</sup>. An equivalent Hamiltonian in a different gauge is

$$H = \frac{1}{2}(p - \epsilon \omega^{-1} \sin \omega t)^2 - \frac{1}{x} \quad (2)$$



The unperturbed classical dynamics ( $\epsilon = 0$ ) possesses a bound-state region in phase space, and the border of this region is a separatrix (trajectory of zero energy). Inside the bound-state region, action-angle variables  $(n, \theta)$  can be introduced. The frequency  $\Omega$  of the unperturbed motion depends on the action  $n$  according to  $\Omega(n) = n^{-3}$  and approaches 0 on the separatrix.

The application of the resonance overlap criterion<sup>6</sup> shows that for any nonzero field strength  $\epsilon$  a *stochastic layer* exists close to the separatrix. Inside this layer the orbits are chaotic and diffuse until they ionize. The thickness of the layer depends on  $\epsilon$  and  $\omega$ . The condition for strong ionization starting from a given bound state is just that the stochastic layer extends so far downwards as to include the given state. Given  $\omega$  and the initial action  $n$ , the critical field strength required for that can be estimated and defines the *classical chaotic threshold*.

### 3.2-The Kepler Map

Following a well known method in the theory of dynamical systems, the continuous time dynamics ruled by the Hamiltonian (1,2) can be analyzed by means of appropriate *Poincare' sections*, that are introduced as follows. First, the time-dependent, 1-freedom problem is transformed into a time independent, 2-freedom problem by introducing a new couple of conjugate variables  $N, \phi$  with  $\phi = \omega t$  ( the phase of the field ). The appropriate Hamiltonian is then

$$\mathcal{H}(p, x, N, \phi) = \frac{1}{2}(p - \epsilon\omega^{-1} \sin \phi)^2 - \frac{1}{x} + \omega N \quad (3)$$

The motion develops on a 3d hypersurface  $\mathcal{H} = \text{const.} = \lambda$ . From (3) it is seen that  $\omega N = \lambda - E$  where  $E$  is the unperturbed energy. The 2d variety  $\sigma$  defined by  $p = 0$  can now be used to construct a Poincare' map. An orbit leaving from a point  $P$  of  $\sigma$  will in general cross again  $\sigma$ ; the first such intersection  $P'$  is taken as the image of  $P$  under the map. Since  $N, \phi$  can be used as canonical coordinates on  $\sigma$ , the map will specify the changes of  $N, \phi$  between subsequent crossings of the variety  $\sigma$ . If  $\epsilon\omega^{-1} \ll 1$ , these crossings occur when  $\dot{x}$  is close to 0, i.e., when the electron is close to the apohelion.

Therefore, roughly speaking the map yields the change in energy between subsequent passages at the aphelion, i.e. it corresponds to a stroboscopic observation of the orbit at intervals of time approximately equal to the (variable) orbital period.

An approximate explicit expression of the map can be easily found<sup>3,7</sup>. This expression is especially simple if the field frequency is much larger than the unperturbed Kepler frequency ( i.e., if  $\omega n^3 \gg 1$  ) \*:

$$\begin{aligned}\bar{N} &= N + k \sin \phi \\ \bar{\phi} &= \phi + 2\pi\omega[2(\omega\bar{N} - \lambda)]^{-3/2}\end{aligned}\quad (4)$$

Here  $k = 0.822\pi\epsilon\omega^{-5/3}$ . The above map is defined only if  $\omega\bar{N} - \lambda \geq 0$ , i.e., only for negative energies. The iteration of the map must be stopped when the energy becomes positive, because then the orbit has ionized. Moreover, the map (4) is the result of a perturbative calculation and is valid only for not too large  $k$  (see ref.3).

Upon linearizing the 2nd eq.(4) around some value of  $N$ , corresponding to a value  $E_0 = -(2n_0)^{-1}$  of the energy, and dropping an unessential constant, one obtains the Standard Map:

$$\begin{aligned}\bar{N} &= N + k \sin \phi \\ \bar{\phi} &= \phi + T\bar{N}\end{aligned}\quad (5)$$

where  $T = 6\pi\omega^2 n_0^5$ . This is a very important result: for *scaled frequency*  $\omega n^3 \gg 1$ , the classical excitation process is locally described by the Standard Map. The resulting picture of chaotic excitation is as follows: the electron moves almost undisturbed along its unperturbed orbit - apart from small field-induced oscillations around it, that do not change its average energy - until it comes close to the nucleus. There it receives a "kick" described by the Standard Map. Above the chaotic threshold, these kicks come at random, and the electron performs a kind of a random walk in energy, until it ionizes.

### 3.3- The Quantum Kepler Map.-

The quantization of the Floquet Hamiltonian (3) is readily accomplished by the standard rule  $N \rightarrow -i \frac{\partial}{\partial \phi}$ . Once quantized, the variable  $N$  will take only integer values; recalling

\* In the present form of the map, the phase  $\phi$  is taken at the perihelion

that  $-\omega N$  coincides with the unperturbed energy, apart from an additive constant, one is naturally led to identify  $N$  with the number of photons.

In the same vein, one can undertake a formal quantization of the Kepler Map (4) and investigate the nature of the discrete-time dynamics defined by the Quantum Kepler Map obtained in this way<sup>3</sup>. One finds that the Quantum Kepler Map is given by an operator acting on state vectors  $\psi(\phi)$  according to:

$$\bar{\psi}(\phi) = e^{-i\hat{H}_0} \hat{P} e^{ik \cos \phi} \psi(\phi)$$

where

$$\hat{H}_0 = 2\pi \left[ -2\omega(N_0 + \hat{N}) \right]^{-1/2}$$

the operator  $\hat{P}$  is the projector on bound states  $N < -N_0 = n_0/2\omega_0$ . This quantum dynamics can be formally described as a motion on a discrete lattice where the sites are labelled by the integer values of  $N$ . This has the following physical meaning. Starting from some initial hydrogenic bound state, and by absorbing or releasing photons, the atom will jump from one state to another in a ladder of 'quasi resonant' bound states ("photonic" states). These states correspond to the sites in the lattice, and the electron can jump from one site to another by absorbing or emitting some photons.

Since the classical map describes the motion only in the bound state region, from which the electron may leave when ionization occurs, the quantum map can account only for the absorption of a maximum number of photons, given by the number of photons required to ionize:  $N_I = (2n_0^2\omega)^{-1}$ . In other words, the quantum map defines the dynamics on a *finite* lattice. The quantum map also includes a dissipation which describes direct ionization: this is active only on a few photonic states close to the 1-photon ionization border.

As can be guessed from the similarity of the classical Kepler map to the Standard Map (5), the Quantum Kepler Map is closely related to the Quantum Kicked Rotator, that will be presently quickly reviewed.

### 3.5 -Localization in the Quantum Kicked Rotator

The quantum kicked rotator is obtained by quantizing the Standard Map (5). Its motion can be formally described as a quantum motion on the discrete, *infinite* lattice defined by the integer values of  $N$  ( that has now the meaning of angular momentum ). This motion is always localized: a wave packet initially concentrated at some site  $N_0$  will start spreading on the lattice, but after a while it will "freeze" into an average steady-state configuration. The corresponding probability distribution over the sites will be fluctuating around an average distribution:

$$f(N) = \frac{1}{2l} \left[ 1 + \frac{2|N - N_0|}{l} \right] \exp \left[ -\frac{2|N - N_0|}{l} \right] \quad (6)$$

where  $l$  is the *localization length*. In the semiclassical regime, and in the region of strong classical chaos, one has the remarkable estimate  $l \approx \frac{1}{2} k^2$ .

The above estimate comes from a very general argument that can be summarized as follows<sup>11</sup>. Let us consider a periodically perturbed quantum system which has a chaotic classical limit. Given the states  $\psi(k)$  of the system after  $k = 1, 2, \dots, N$  periods of the perturbation, we can investigate the quasi-energy spectrum by performing a discrete-time Fourier analysis of their string  $c_k = \langle \psi(0) | \psi(k) \rangle$  where  $\langle \cdot | \cdot \rangle$  is the scalar product. Given  $c_k$  up to  $k = N$ , we can resolve the spectrum on a scale  $\sim \frac{1}{N}$ . On the other hand we can expect the number of frequencies significantly contributing in the motion up to time  $N$  to be on the same order as the number of unperturbed levels excited up to the same time; this number is roughly  $\Delta n \approx (DN)^{\frac{1}{2}}$  with  $D$  the classical diffusion coefficient. Therefore, on the scale  $1/N$  the quasi energy spectrum will be resolved by just  $(DN)^{\frac{1}{2}}$  values. This means that for sufficiently large  $N$  gaps will appear in the spectrum, roughly for  $\bar{N} \approx (DN)^{\frac{1}{2}}$ , i.e., for  $\bar{N} \approx D$ . For such  $\bar{N}$  recurrences should be expected to appear and to slow down the excitation. The spread  $\Delta n$  of the wave packet at the same time  $\bar{N}$  will be on the order of the maximum spread attainable by the wave packet in the course of its evolution; since the latter is just given by the localization length, we get  $l \approx D \approx k^2/2$  where the latter estimate is well known and comes from estimating the classical diffusion coefficient under a random phase assumption that is very well justified in the case of strong classical chaos.

### 3.5 -Localization in the H-atom

The dynamical localization theory for the Hydrogen atom in a microwave field is basically an extrapolation to that problem of the results obtained for the quantum rotator ( QKR ), a bridge being provided by the Quantum Kepler Map ( QKM ). This extrapolation rests on some assumptions:

- that the QKM is in some sense an approximation for the real Schrodinger equation. This is by no means obvious: the connection between the discrete time defined by the number of iterations of the Map and the real time is quantum- mechanically lost as soon as the wave packet spreads over states which have significantly different classical orbital periods.
- that the similarity in structure between the QKR and the QKM justifies the application to the QKM of known results about the QKR. The essential difference between the QKM and the QKR is that the former lives in a *finite* lattice. and that this lattice has a 'leaky end' due to direct ionization from photonic states close to the ionization border. Nevertheless, as long as the wave packet does not significantly populate these border states, the dissipation can be neglected and the QKM and QKR dynamics will be similar - in their gross features at least. This will certainly be the case if  $l \ll N_I$ , because the wave packet will "freeze" before having a chance to significantly populate the border sites. Since as explained above  $l \approx k^2/2$  for the KR and the "kick strength" of the Kepler Map is  $k = 0.0822\pi\epsilon\omega^{-5/3}$ , one should expect the localization length in the number of photons to be given by

$$l = 3.33\epsilon^2\omega^{-10/3}$$

which is well confirmed not only by the numerical simulation of the quantum Kepler Map but even by the numerical solution of the Schrodinger equation (Figs.1), thus fully supporting the validity of the Kepler Map approach also for the quantum problem. Given this explicit formula for  $l$ , the condition for localization  $l \ll N_I$  takes the form:

$$\epsilon < \epsilon_q = \frac{\omega_0^{7/6}}{(6.6n_0)^{1/2}} \quad (7)$$

There is a wide range of parameters where this condition can be satisfied while keeping the field strength well above the classical chaos border. In this region, a phenomenon of dynamical localization quite similar to the one observed in the QKR will prevent the atom from ionizing so fast as it should classically. The "frozen" distribution will have the form (6) with  $N$  the number of absorbed photons.

### 3.5-Delocalization

If  $l$  is increased ( e.g., by increasing the field strength ) while keeping  $N_I$  constant, the above picture will lose its validity. Qualitatively one can expect the ionization rate to increase due to the onset of a diffusive excitation more or less like the classical one. Conditions for this are that  $l \gg N_I$  and that at the same time  $k \ll N_I$  ( implying that a large number of kicks are needed to ionize ).

### 3.8- Numerical Checks

The localization phenomenon for the H-atom in a microwave field has been confirmed by extensive numerical simulations of the time-dependent Schrodinger equation since 1984<sup>2</sup>. In addition to that the Kepler map yields an indication of great heuristic value, namely that the shape of the localized distribution should be exponential in the number of absorbed photons ( formula (6) ). This has also been confirmed by numerical computations<sup>3</sup>. In fig 1 an example is shown of localized distributions obtained from the numerical integration of the Schrodinger equation. The distribution over the unperturbed hydrogenic states (labelled by the quantum number  $n$ ), suitably averaged in time, is plotted ( in logarithmic scale ) versus the number of absorbed photons  $N = (2n^2)^{-1} - (2n_0^2)^{-1}$  where  $n_0 = 100, 200$  is the quantum number of the initially excited state. Here  $\omega n_0^3 = 3.5$ . The exponential character of the distribution is fairly evident, as well as the role of the quasi resonant 'photonic' states.

### 3.9- Beyond the 1d Model

Although the above theory was developed for the 1-dimensional model, its predictions turn out to be valid even for more realistic situations. As we already mentioned, the experimentally observed ionization thresholds could be satisfactorily reproduced by numerical simulation of 1d classical models; on qualitative grounds, it was held that almost one dimensional orbits, i.e. orbits very elongated in the field direction could be more easily ionized so that they would give a dominant contribution to the ionization rate in the threshold region.

We have investigated a two-dimensional model in which the magnetic quantum number with respect to the field direction is 0. We were able to find a Kepler Map that approximately describes the changes of the canonical variables  $N, \mathcal{L}, \phi, \psi$  between subsequent passages at the aphelion;  $\mathcal{L}$  is angular momentum, and  $\psi$  its conjugated phase. Although this map is quite complicated<sup>3</sup>, an approximated analysis shows that the evolution of elongated orbits is essentially one-dimensional - i.e., it develops as predicted by the 1d model - due to the existence of an approximate integral of motion. Over not too long times ( on the order of the experimental interaction times ) the two degrees of freedom behave as if they were uncoupled. This theoretical argument in support of the validity of the 1d model even in 2d situations was confirmed by numerical simulations of a quantum 2d atom, that yielded evidence of an exponential localization in the number of photons quantitatively similar to the one occurring in the 1d model (Fig.2).

### 3.8-Experimental Verifications.-

Experimental results on microwave ionization of highly excited Hydrogen atoms in the region  $\omega n_0^3 > 1$  were reported for the first time in 1988 by Galvez *et al*<sup>9</sup>. Until then, numerical computations and experiments in the region  $\omega n_0^3 < 1$  had shown that classical mechanics accounts very well for most of the experimental results. The 1988 experimental data clearly show that in the high-frequency region the quantum ionization thresholds rise above the classical ones. These data provide experimental evidence for

the quantum suppression phenomenon. This was confirmed by new experiments by another experimental group in 1989; in this case, the experimental results were also found to agree with some quantitative predictions of localization theory<sup>10</sup>.

A typical microwave ionization experiment produces "ionization curves" like those shown in Fig.3, which displays some of the experimental data by Galvez *et al.* For given  $\omega$  and  $n_0$  the field strength is increased until 10percent ionization is achieved. The corresponding value of the 'scaled field'  $\epsilon_0 = \epsilon n_0^2$  is plotted versus the 'scaled frequency'  $\omega_0 = \omega n_0^2$ ; the latter is varied by changing  $n_0$ . The data in Fig.3 were obtained with  $\omega = 36.02$  GHz. Fig.3 shows that for  $\omega_0 > 2$  the 10percent experimental thresholds ( circles ) lie systematically above the ( numerically computed ) classical thresholds ( the crosses in Fig.3 ).

A crucial remark is that the experimentally measured ionization does not only include those electrons that have escaped into the continuum, but also those excited above some cutoff level  $n_c$  ( for a detailed discussion see ref.5). Thanks to this fact, the localization theory can sometimes produce a quantitative estimate for the thresholds. This is the case when only a small part of the total probability flows into continuum in the given interaction time. In that case, (i) the 'ionization probability'  $P$  will be essentially given by the total probability on the bound states above the cutoff  $n_c$ , and (ii) the final distribution over the photonic states will be of the form (6). Therefore,  $P$  can be computed from the distribution (6). In principle, this procedure can be reversed in order to find what the field strength must be, in order that  $P = 0.1$ . This yields a simple formula<sup>11</sup> which corresponds to the smooth line in Fig.3. More precisely, if we define the ionization probability as the total probability above a fixed level  $\bar{n}$ , the threshold for 10% ionization is obtained from the condition

$$0.01 = \int_{\bar{N}}^{\infty} f(N) dN$$

with  $\bar{N} = (n_0^{-2} - \bar{n}^{-2})/2\omega$ . The rhs of the last eqn. can be computed as a function of  $\epsilon$  by using eqn(6), and the resulting equation can be solved for  $\epsilon$ .

However, in order that this procedure be a self-consistent one, the field strength and the localization length found in this way must not be so large as to significantly



populate the fast-ionizing states close to the ionization border; otherwise, the dissipation cannot be assumed to be small. In such a case the 'localization formula', which does not account for continuum, cannot be used - it would be found to overestimate the actual thresholds. For instance, this will happen if the cutoff  $n_c$  is pushed very far from the initially excited state - it will not be possible in that case to transfer a 10percent probability on the bound states beyond the cutoff, without populating the border states. One such case that lies beyond the limits of applicability of the localization formula was reported in refs 5,9.

A further confirmation of the localization effect was provided by experimental work of J.Bayfield and D.W.Sokol<sup>10</sup>. This work was especially designed in order to check the predictions of localization theory and was carried out in close parallel with numerical simulations of the experimental setup. Whereas in the case of Galvez *et al.* atoms were prepared in a microcanonical distribution of states with a given principal quantum number, in Bayfield's case the magnetic quantum number along the direction of the field could be assumed to be zero; the situation here was therefore "two-dimensional" as compared to the "three-dimensional" situation of Galvez *et al.* Another point of difference was that the microwave interaction took place inside a wave guide ( Galvez *et al* had a microwave cavity instead ) where atoms were exposed to a microwave pulse of frequency varying in a band 12.4 to 18 GHz, with a nominal envelope  $\sin(t/7.5nsec)$ . Finally, a static field 0.87 Volt/cm was superimposed to the microwave field; this field would have produced static-field ionization of states with principal quantum number 164, considerably higher than the adjustable cutoff level  $\bar{n}$  used to empirically define ionization.

Figure (4) shows thresholds for 10% ionizations obtained experimentally, by quantum numerical simulations on the 1d model, and by the above sketched theoretical formula. ( solid line ). To be emphasized is that the theory does not describe either quantum or classical resonance effects, as it is based upon only the smoothed behaviour of stationary state distributions in quantum number.

#### 4.- HIGHER DIMENSIONAL LOCALIZATION

How can the localization effect be circumvented? In the theory of Anderson localization in disordered solids this question admits of a variety of different answers, depending on the spatial dimension of the solid themselves. In the one dimensional case, i.e. for a solid shaped like a bar or a wire, the localization becomes ineffective as soon as the localization length becomes larger than the length of the solid. The delocalization in the H-atom problem has the same origin: here the length of the "solid" is defined by the number of photons that will carry the electron into the continuum ( see the discussion in Sec.1.1.2) , and the condition that this length be smaller than the localization length is just eqn.(7). For two- and three-dimensional solids, besides this obvious finite-sample effect, other mechanisms exist that make the effect of Anderson localization milder. It is a natural question whether these higher-dimensional localization effects have a dynamical counterpart, too.

As summarized above, the dynamics of a quantum system subjected to a perturbation periodic in time is formally "conjugate" to a one-dimensional localization problem. It turns out that higher dimensional localization problems have a dynamical counterpart in the dynamics of systems subjected to a number of incommensurate frequencies. Notice that the Kicked Rotator is subject to infinitely many frequencies *commensurate* frequencies given by the integer multiples of the kick frequency and that the hydrogen atom is subject to a monochromatic field. It is known[4] that the addition of a second incommensurate frequency in the kicked-rotator model does not destroy the localization effect; nevertheless, the localization lengths are sharply increased in comparison to the one frequency case, in a way that somehow reproduces known results from the theory of 2-d disordered solids ("films").

The most interesting case is the one with *three* incommensurate frequencies. As we shall presently explain, this corresponds to a three dimensional localization problem. According to the theory of Anderson localization a transition from localized to extended states should be expected as the coupling strength is varied. The reason why

investigating the possibility of a similar transition in a dynamical model is important is twofold. First, one needs to ascertain whether the localization effects that prevents diffusive excitation can be circumvented, so that in some cases at least quantum systems can prove as unstable as their classical counterparts are. Second, the precise details of the Anderson transition are not yet completely understood; the theoretical analysis is complicated and the numerical simulation prohibitive. In contrast, the numerical analysis of dynamical models is much less expensive; as a matter of fact, in this way we were able to obtain some interesting indications at a relatively low computational cost<sup>12</sup>.

#### 4.1- Anderson Transition in a Dynamical Model

We studied the motion of a particle on a circle, described by the time-dependent Hamiltonian:

$$H = H_0 + V(\theta, t) \sum_{s=-\infty}^{+\infty} \delta(t-s) \quad (8)$$

The 2nd term describes kicks occurring periodically in time with period one. The free evolution between kicks is given by the Hamiltonian  $H_0$ :

$$H_0|n\rangle = E_n|n\rangle, \quad |n\rangle = (2\pi)^{-1/2} \exp(in\theta)$$

We assume the eigenvalues  $E_n$  to be random numbers uniformly distributed in  $(0, 2\pi)$ .

We also assume  $V$  to explicitly depend on time according to

$$V = V(\theta, \theta_1 + \omega_1 t, \theta_2 + \omega_2 t)$$

with  $V$  a periodic function of its three arguments to be specified later, and  $\theta_{1,2}$  arbitrarily prescribed phases. Since we would like  $\omega_{1,2}$  to be incommensurate with each other and also with the frequency of the kicks, we take  $\omega_1 = 2\pi\lambda^{-1}$  and  $\omega_2 = 2\pi\lambda^{-2}$  with  $\lambda = 1.3247\dots$  the real root of the cubic equation  $x^3 - x - 1 = 0$ . With such a choice,  $\omega_{1,2}$  are a 'most incommensurate' pair of numbers. The evolution of the system from just after one kick to just after the next is given by ( we take here  $\hbar = 1$  ):

$$\psi(\theta, t+1) = e^{-i\lambda^{-1}(\theta, t+1)} e^{-iH_0} \psi(\theta, t) \quad (9)$$

Expressed in this form, the rotator dynamics is very easily simulated because the time dependence of  $V$  is explicitly known.

We shall now elucidate how is this model connected with a 3d tight-binding model of the Anderson type. First of all we consider the phases  $\theta_{1,2}$  as new dynamical variables, with conjugate momenta  $n_{1,2}$ . Then we consider the Hamiltonian

$$H' = H_0(\hat{n}) + \omega_1 \hat{n}_1 + \omega_2 \hat{n}_2 + V(\theta, \theta_1, \theta_2) \sum_{s=-\infty}^{+\infty} \delta(t-s) \quad (10)$$

with  $\hat{n}_{1,2} = -i\partial/\partial\theta_{1,2}$ . The last hamiltonian describes a rotator with three freedoms  $\theta, \theta_1, \theta_2$  subjected to periodic kicks, the strength of which is no more time dependent. The one-period propagator for this rotator is now

$$e^{-iV(\theta, \theta_1, \theta_2)} e^{-i[H_0(\hat{n}) + \omega_1 \hat{n}_1 + \omega_2 \hat{n}_2]} \quad (11)$$

In order to recognize that the 3d quantum model defined by (10) and the 1d model defined by (8) are substantially equivalent, it suffices to rewrite the Schrodinger equation for the 3d model,

$$i \frac{d}{dt} \psi(\theta, \theta_1, \theta_2, t) = H' \psi(\theta, \theta_1, \theta_2, t)$$

in the interaction representation defined by

$$\psi(\theta, \theta_1, \theta_2, t) = e^{-i(\omega_1 \hat{n}_1 + \omega_2 \hat{n}_2)} \bar{\psi}(\theta, \theta_1, \theta_2, t)$$

In this way, one immediately recovers the Schrodinger equation with Hamiltonian (8) for the wave function  $\bar{\psi}$ .

We can now apply to the 3-rotator (10) a well-known transformation<sup>1</sup> that will map it onto a 3d tight-binding model. Thanks to this transformation, the problem of determining the quasi-energy eigenvalues and eigenvectors of the 3-rotator will be turned into the problem of solving the equation:

$$T_n u_n + \sum_{r \neq 0} W_r u_{n+r} = \epsilon u_n \quad (12)$$

where  $n = (n, n_1, n_2)$  and  $r$  label sites in a 3d lattice,

$$T_n = -\tan[0.5(E_n + n_1\omega_1 + n_2\omega_2 + \lambda)]$$

Here  $\lambda$  is quasi-energy,  $W_r$  are the coefficients of a threefold Fourier expansion of  $\tan[0.5V(\theta, \theta_1, \theta_2)]$  and  $\epsilon = -W_0$ . We now choose

$$V(\theta, \theta_1, \theta_2) = -2\arctan[2k(\cos\theta + \cos\theta_1 + \cos\theta_2)]$$

and eqn.(12) becomes

$$T_n u_n + k \sum_r u_r = 0$$

where the sum includes only nearest neighbours to  $n$ .

After all these formal manipulations, the original rotator problem has been turned into a tight-binding model of the Anderson type; the nature of the eigenstates of the latter will determine the nature of the dynamics of the rotator, that will be localized or delocalized ( in the sense of unbounded excitation taking place ) according to whether these eigenfunctions are localized or extended. The disorder in the model (12) is given by the pseudorandom character of the potential  $T_n$ .

The model was investigated by numerically simulating the dynamics of the rotator, starting with the same initial state and with increasing values of the coupling constant  $k$ . A transition between two types of motion was detected around a value  $k_{cr} \sim 0.47$ , the dynamics being localized for  $k < k_{cr}$  and delocalized for  $k > k_{cr}$ . In the former case the ( time-averaged ) steady-state distributions were found to be exponential (Fig.5) and the corresponding localization lengths could be determined. In the latter, unbounded diffusive excitation occurs, with Gaussian-like distribution of width linearly increasing with time (Fig.6) , so that the diffusion coefficients could be determined. A remarkable result was obtained from the analysis of the behaviour of the inverse localization length  $\gamma$  and of the diffusion coefficient close to the transition point (Fig.7): we found that

$$D \sim \text{const.} |k - k_{cr}|^s, \quad \gamma \sim \text{const.} (|k - k_{cr}|)^\nu$$

with  $s \sim 1.25$  and  $\nu \sim 1.5$ , which are close to values theoretically obtained in localization theory from diagrammatic computations.

This result of ours enforces a striking similarity between the dynamics of quantum systems under almost periodic perturbations and tight-binding models with spatial dimension given by the number of incommensurate frequencies.

### 3.- CONCLUSIONS AND RECOMMENDATIONS

The core of the research activity summarized in this final report was the development of the *dynamical localization theory* and its application to a specific problem in atomic physics. Originally motivated by a theoretical interest in the possible survival of effects of classical stochasticity in quantum mechanics, this research has brought into the light a class of generic behaviours of small quantum systems subjected to periodic perturbations such as, e.g., atoms and molecules in external fields. The excitation of such systems is strongly limited by a coherence effect that is basically the same that is responsible for the Anderson localization in solid state physics; by generalizing some typical concepts and methods of the theory of Anderson localization, we were able to get a simple albeit rough quantitative description of the excitation of atoms in microwave fields that has stood the test of laboratory experiments. The dynamical localization theory has predicted the quantum suppression of diffusive ionization that was first confirmed by numerical simulations and then observed in laboratory.

Notwithstanding this undoubted success, much work has still to be done. Although already in its present form the theory represents a statistical, non-perturbative approach that can prove useful in a variety of time-dependent problems, more theoretical work is needed in order to completely understand how does localization stem out of the Schrodinger equation. Even more important, the firmly established similarity of the dynamical localization with the better known Anderson localization opens the way to further exciting developments.

As we have emphasized several times in this report, the predictions of our theory are essentially statistical, as a result, the agreement with experimental data holds only "in the average". Indeed both the numerical and the experimental data exhibit more or less relevant deviations from the average theoretical prediction. This is hardly surprising, because the dynamical localization theory was just meant to yield a gross description of the quantum dynamics; actually, as it was pointed out in ref<sup>3</sup>, one would expect even stronger fluctuations than were actually observed. Indeed, according to the theory, the

quantum distribution is strongly fluctuating around its average exponential shape, and these fluctuations will affect, also the ionization rate which will have a very irregular fine structure .

Short of representing a failure of our theoretical approach, these "fluctuations" are an essential part of the theoretical picture of localization theory and in the case of Anderson localization their statistical description is a major goal of the theory . They are not due to uncontrolled changes in the environment or to any form of external noise; they are perfectly reproducible, so that in principle the very use of the word "fluctuations" might be questioned. Though these irregularities stem from purely quantum coherence effects - nothing comparable is to be found in the classical ionization rates -, it may well be the case that the seemingly irregular structures that characterize the ionization curves correspond to identifiable structures in the classical phase space ( "scars" ). Nevertheless, an individual description of such local structures appears hardly feasible. Although there have been isolated successes in associating some quantum details with classical objects such as periodic orbits or "homoclinic tangles" , , this kind of classical structures are of course individually unpredictable, as is for the time being the mechanism why some of them find sometimes their way to "scarred" quantum states.

Therefore, from a physical standpoint, a statistical approach is recommended, aimed at quantitatively describing how do these irregular variations of ionization rates scale with the relevant parameters.

On more general grounds, these "fluctuations" are but one more instance of a sensitive dependence of quantum reaction rates on various parameters that has been observed in several areas, from nuclear physics to solid state. Some universal characteristics are now emerging, that are conveniently modelled by Random Matrix Theory, and many investigators of these different fields are now adopting as a working hypothesis that a unified approach at such different, purely quantum "fluctuation" phenomena may be based on the chaotic nature of the underlying classical mechanics. Insofar as future work is concerned, we believe that just this one is the most promising indication of the work we have been summarizing in this report.

## 5.- FIGURE CAPTIONS

Fig.1- Probability distribution over the unperturbed levels averaged from 450 to 500 microwave periods (full curve) versus the number of photons  $N_\phi$  for  $\epsilon_0 = 0.03, \omega_0 = 3.5$ . The straight line results from a least squares fitting of the maxima of the distribution in each photon interval. The dots give the steady state distribution obtained by iterating the quantum map. (a)  $n_0 = 100$ , (b)  $n_0 = 200$ . For comparison, the classical distribution over unperturbed levels is also shown in (b) (dashed curve) (From ref.(3)).

Fig.2- Classical (dashed curve) and quantum (full curve) distribution functions versus the number of absorbed photons and for the 2-dimensional model. The straight dotted line is the one-dimensional quantum theoretical exponential distribution; the dotted-dashed line is the analytical solution of the diffusion equation.

Fig.3- Scaled 10% threshold fields from ref.(9). The dashed line is the quantum theoretical prediction according to dynamical localization theory.

Fig.4- A point by point comparison of experimental and quantum mechanical values for the microwave field strength for 10% ionization probability, as a function of microwave frequency. The field and frequency are scaled according to  $\omega_0 = \omega n_0^3, F_0 = \epsilon n_0^4$ . The theoretical points are shown as solid triangles. The experimental points are connected by a dashed curve drawn through the entire data set. Values of the initial level  $n_0$  and of the cutoff level  $\bar{n}$  are: full circles, 64/114; crosses, 68/114; open circles, 71/114; squares, 80/120; triangles, 86/130; plusses, 94/130; diamonds, 98/130. The dotted line is the classical chaos border; the solid curve, the quantum border.

Fig.5- Example of a localized steady-state distribution over the unperturbed levels of the three-frequencies model, averaged over 5000 iterations in the interval 95000;100000. Here  $k = 0.38$ .

Fig.6. Example of a Gaussian distribution over the unperturbed levels in the delocalized regime of the three-frequencies model. The distribution is averaged over 1000 iterations in the interval 19000;20000.



Fig.7.- Diffusion rate  $D$  (dots) and inverse localization length  $\gamma$  as functions of the coupling strength  $k$ . Error bars were obtained from statistics over ten different realizations of the random spectrum. The dotted lines result from a 3-parameters least squares fit.

## 6.-BIBLIOGRAPHY

- [1] S.Fishman, D.R.Grepel, R.E.Prange, Phys.Rev.Lett. 49,509 (1982).
- [2] G.Casati, B.V.Chirikov, D.L.Shepelyansky and I.Guarneri, Phys.Rep. 154, 77 (1987).
- [3] G.Casati, I.Guarneri and D.L.Shepelyansky, IEEE J.Quantum Electron. 24 , 1240 (1988).
- [4] D.L.Shepelyansky, in *Chaotic Behavior in Quantum Systems*, G.Casati ed., ( Plenum, NY 1985 ),p.187.
- [5] P.Koch, preprint 1990, to appear in the AIP Conference Proceedings Series.
- [6] R.V.Jensen, Phys.Rev. A30, 386 (1984).
- [7] V.Gontis and B.Kaulakys, J.Phys. B20, 5051 (1987).
- [9] E.J.Galvez, B.E.Sauer, L.Moorman, P.M.Koch and D.Richards, Phys.Rev.Lett. 61, 2011 (1988).
- [10] J.E.Bayfield, G.Casati, I.Guarneri and D.W.Sokol, Phys.Rev.Lett. 63, 364 (1989).
- [11] G.Brivio, G.Casati, L.Perotti and I.Guarneri, Physica D 33, 51 (1988).
- [12] G.Casati, I.Guarneri and D.L.Shepelyansky, Phys.Rev.Lett.62,4 (1989)
- [13] G.Casati, I.Guarneri and D.L.Shepelyansky, Physica A163 (1990), 205
- [14] G.Casati, I.Guarneri and D.L.Shepelyansky, Phys.Rev. A36 (1987) 3501.
- [15] G.Casati, I.Guarneri, F.Izrailev and R.Scharf, Phys.Rev.Lett. 64 (1990) 187.
- [16] U.Smilansky, in *Chaos and Quantum Physics*, M.J.Giannoni, A.Voros and J.Zinn-Justin eds., 1990 ( Lect. Notes for the Les Houches Summer School, session LII, 1989), and references therein.
- [17] J.L.Pichard, J.Phys. C: Solid St. Phys., 19 (1986) 1519.
- [18] M.C.Gutzwiller, Physica D7 (1983) 341.
- [19] T.A.Brody,J.Flores,J.B.French,P.A.Mello,A.Pandey and S.S.M.Wong, Rev.Mod.Phys. 53 (1981) 385.
- [20] B.L.Al'tshuler and P.A.Lee, Physics Today, Dec 1988.
- [21] see, e.g., D.Vollhardt, Festkorper Probleme 27 (1987) 63, and references therein.

[22] J.L.Pichard, in *Quantum Coherence in Mesoscopic Systems*, B.Kramer ed., NATO ASI series, Plenum 1990.

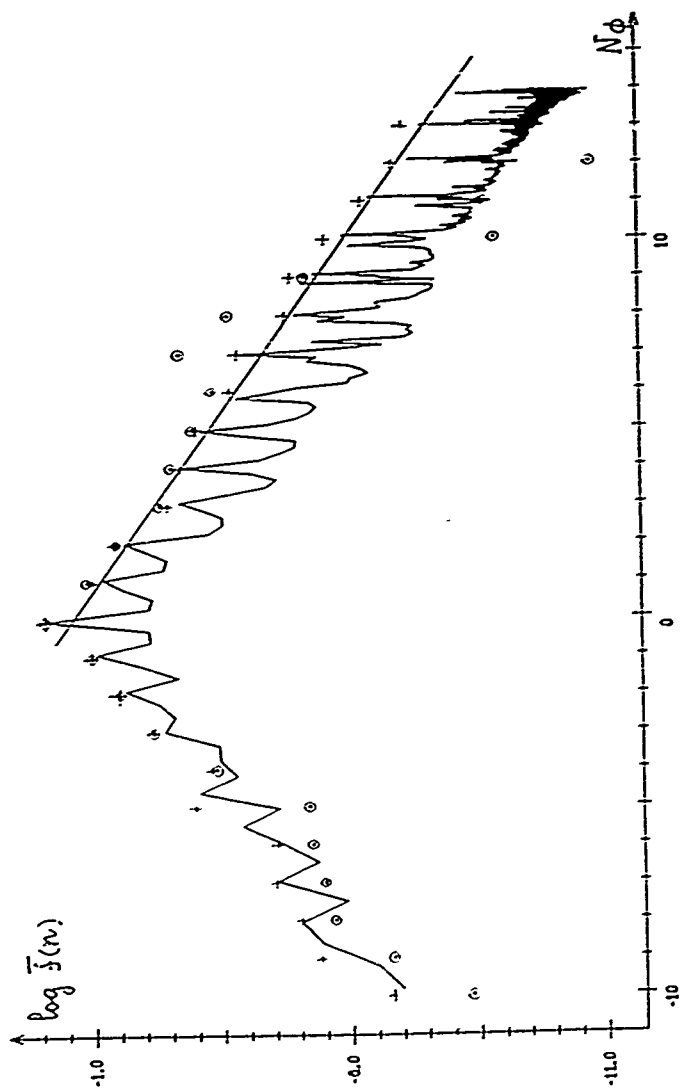


Fig. 1a

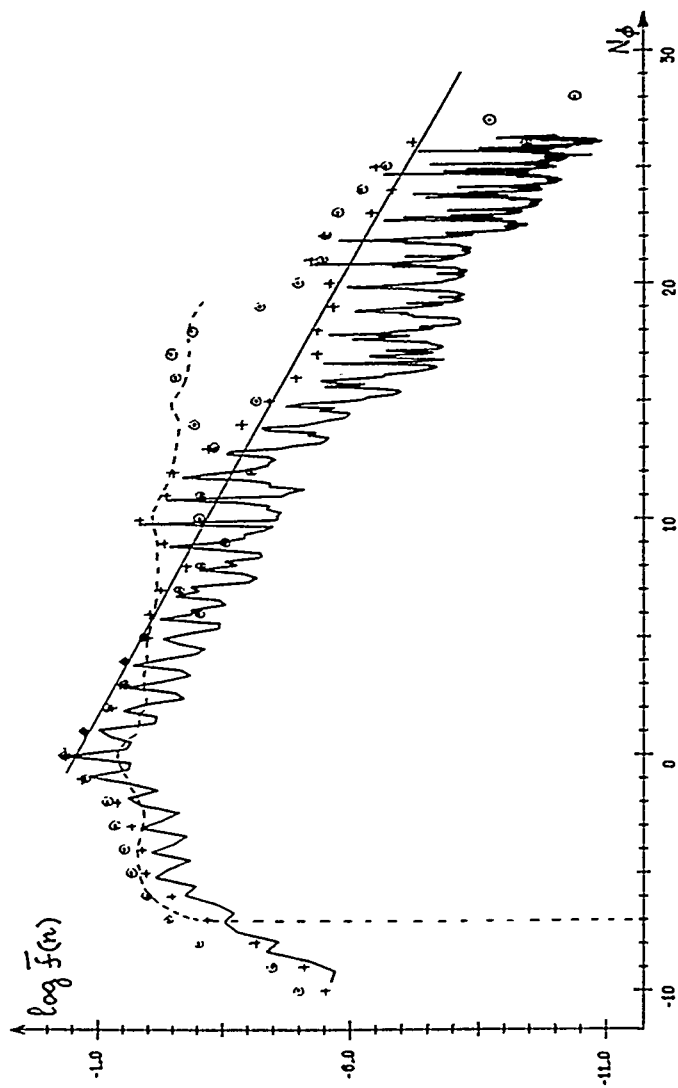


Fig. 1b

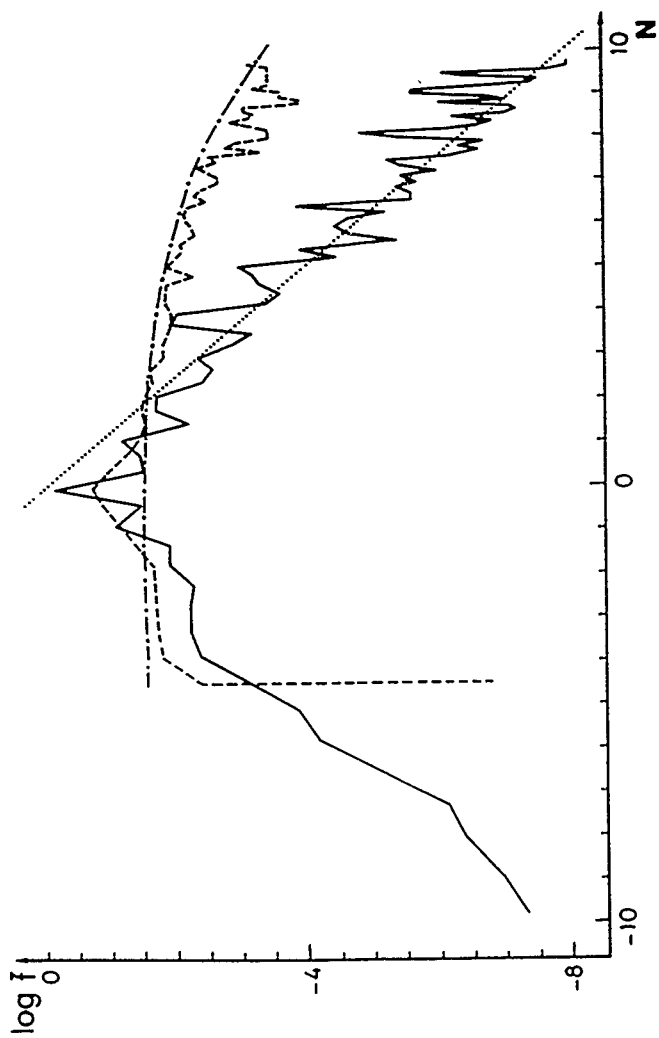


Fig. 2

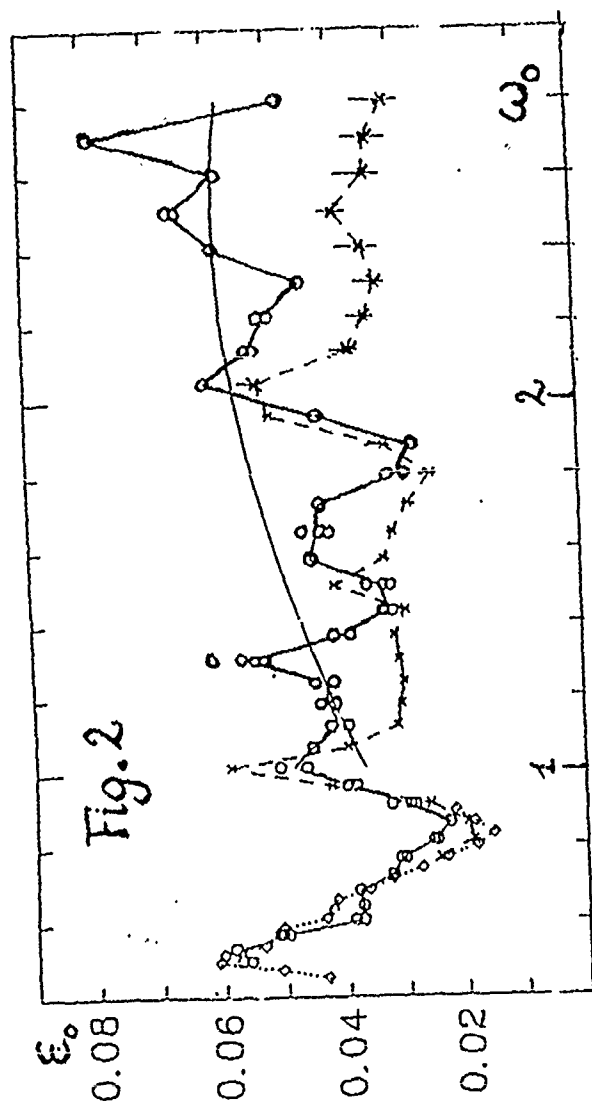


FIG. 3

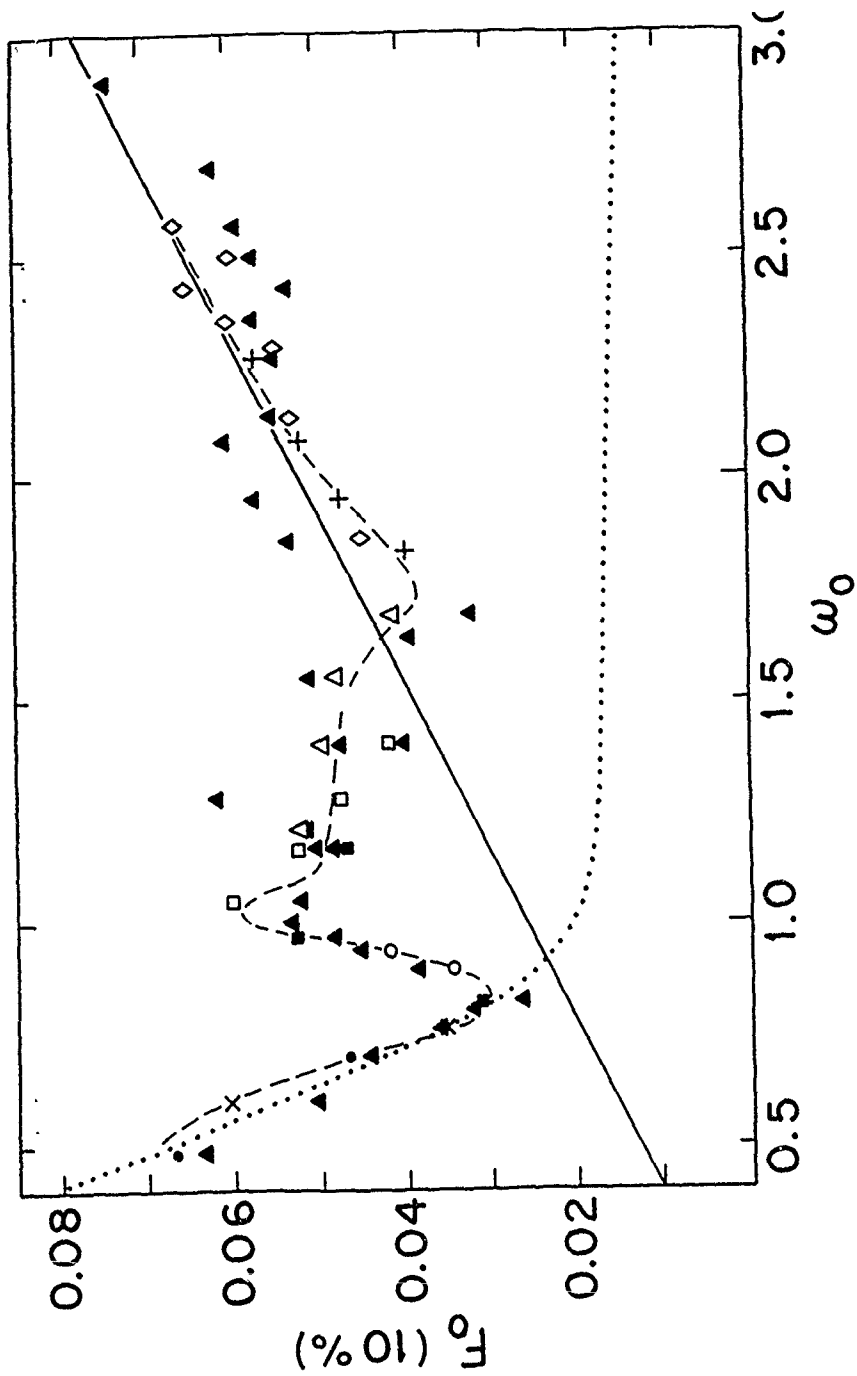


Fig. 4



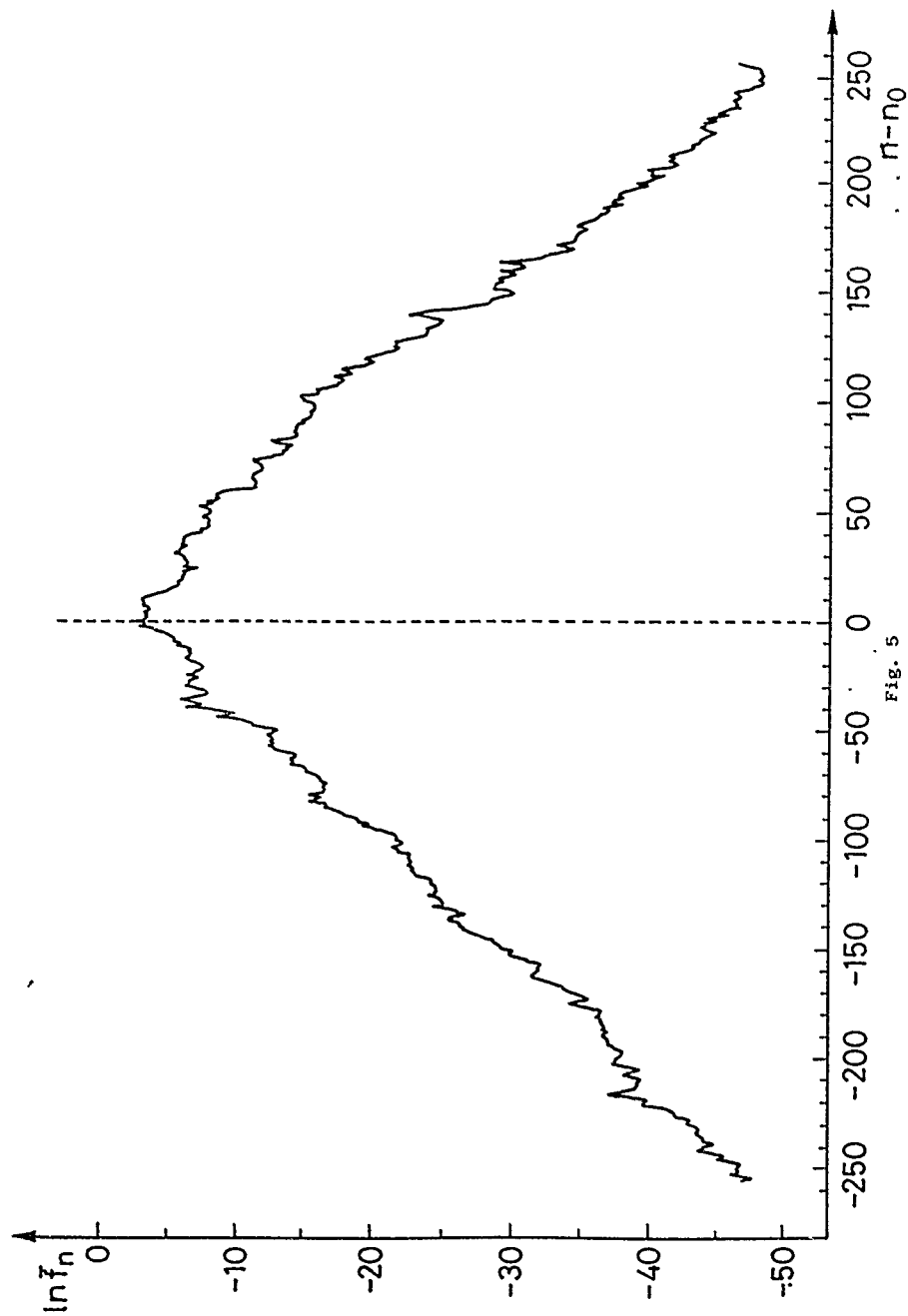


Fig. 5

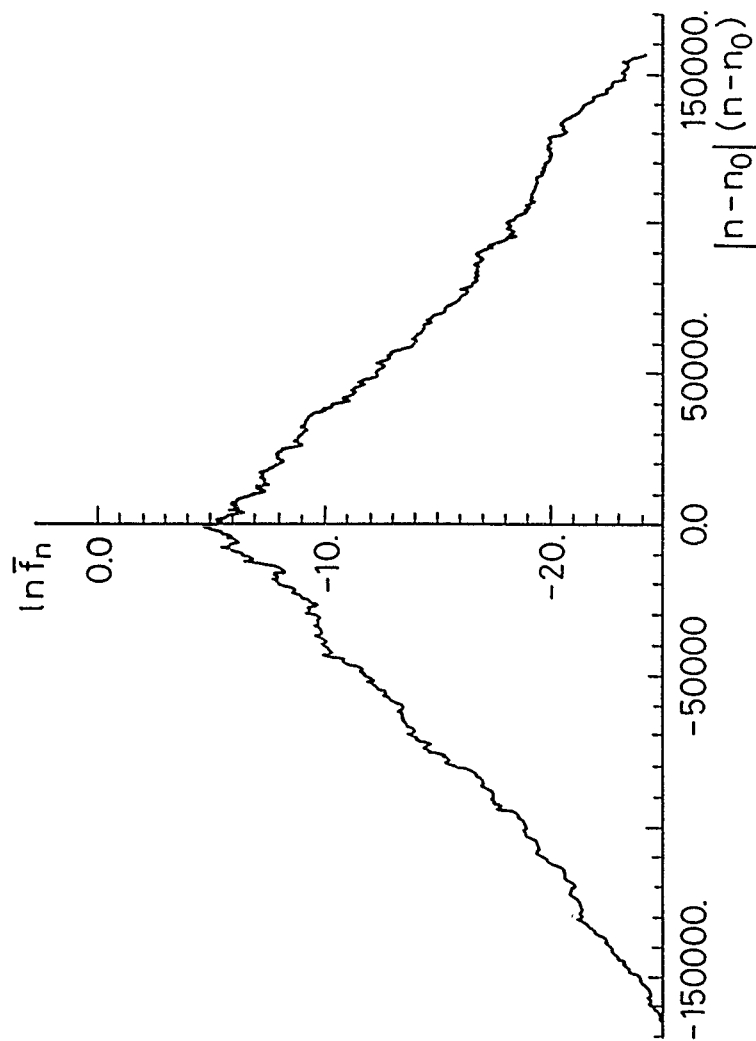


Fig. 6

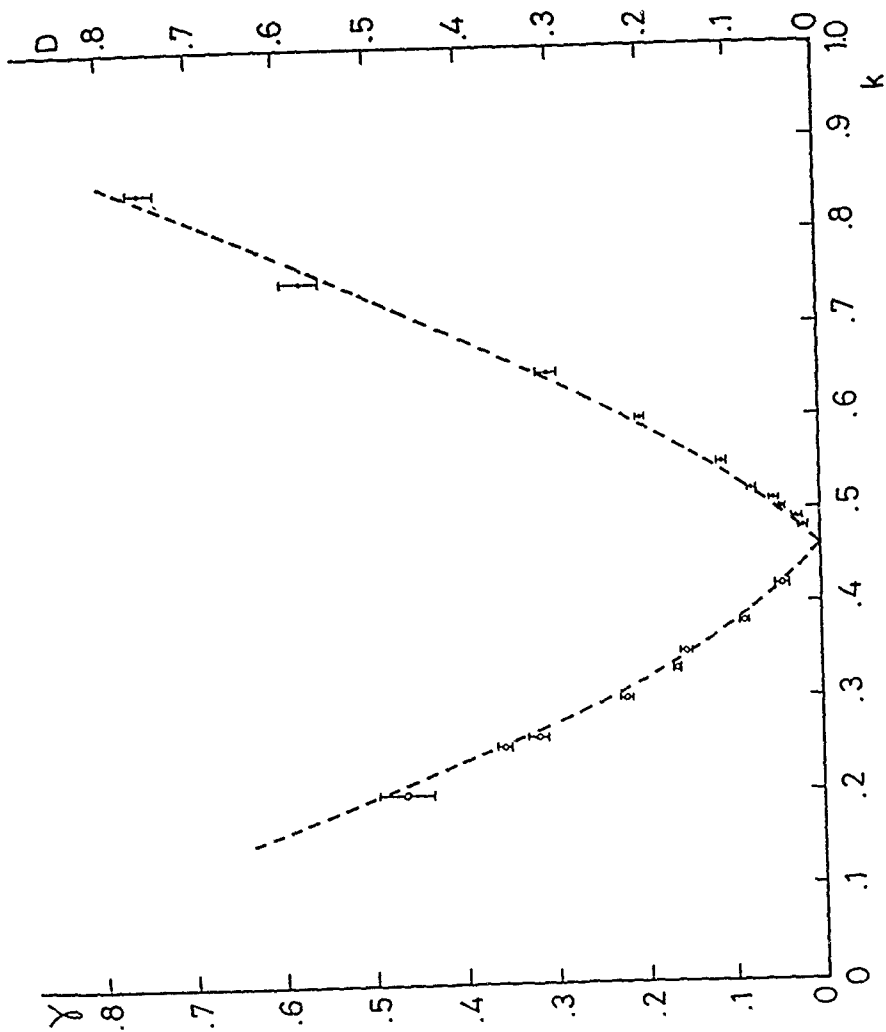


Fig. 7